HHS Public Access

Author manuscript

Int J Radiat Oncol Biol Phys. Author manuscript; available in PMC 2019 November 15.

Published in final edited form as:

Int J Radiat Oncol Biol Phys. 2018 November 15; 102(4): 1255–1264. doi:10.1016/j.ijrobp.2018.05.051.

Correlation of Functional Lung Heterogeneity and Dosimetry to Radiation Pneumonitis using Perfusion SPECT/CT and FDG PET/CT Imaging

Howard J. Lee Jr[1], **Jing Zeng**[2], **Hubert J. Vesselle**[3], **Shilpen A. Patel**[2], **Ramesh Rengan**[2], and **Stephen R. Bowen**[2,3]

[1]Duke University School of Medicine, Durham, NC 27710, USA

[2]Department of Radiation Oncology, University of Washington School of Medicine, Seattle, WA 98195, USA

[3]Department of Radiology, University of Washington School of Medicine, Seattle, WA 98195, USA

Abstract

Purpose: To apply a previously designed framework for predicting radiation pneumonitis, using pre-treatment lung function heterogeneity metrics, anatomic dosimetry, and functional lung dosimetry derived from two imaging modalities within the same cohort.

Materials and Methods: Treatment planning CT scans were co-registered with pre-treatment [^{99m}Tc]MAA perfusion SPECT/CT scans and [^{18}F]-FDG PET/CT scans of 28 patients who underwent definitive thoracic radiation. Clinical radiation pneumonitis was defined as grade ≥ 2 (CTCAE v4). Anatomic dosimetric parameters (MLD, V20) were collected from treatment planning scans. Baseline functional lung heterogeneity parameters and functional lung dose-volume parameters were calculated from pre-treatment SPECT/CT and FDG PET/CT scans. Functional heterogeneity parameters calculated over the tumor-subtracted lung included skewness, kurtosis, and coefficient of variation from perfusion SPECT and FDG PET, as well as global lung parenchymal glycolysis (GLPG) and SUV_{mean} from FDG PET. Functional dose-volume parameters calculated in regions of highly functional lung, defined on perfusion (p) or SUV (s) images, included mean lung dose (pMLD, sMLD) and volume receiving ≥ 20 Gy (pV20, sV20). Fraction of integral lung function receiving ≥ 20 Gy (pF20, sF20) was also calculated. Equivalent doses in 2 Gy per fraction were calculated to account for differences in treatment regimens and dose fractionation ($EQD2_{Lung}$).

Results: Two anatomic dosimetric parameters (MLD, V20) and four functional dosimetric parameters (pMLD, pV20, pF20, sF20) were significant predictors of grade ≥ 2 pneumonitis (AUC > 0.84, $p < 0.05$). Dose-independent functional lung heterogeneity metrics were not associated

Corresponding author and author responsible for statistical analyses: Stephen R. Bowen, PhD, DABR, 206-543-6559, srbowen@uw.edu, 1959 NE Pacific St, Box 356043, Seattle, WA 98195.

CoI statement:

Howard J. Lee Jr. was funded by the RSNA Research Medical Student Grant for this study and this report is submitted to the IJROBP under the policies of this grant. Jing Zeng and Stephen Bowen report grants from the National Cancer Institute, during the conduct of the study. Hubert Vesselle reports grants from Philips Healthcare, outside the submitted work. Ramesh Rengan and Shilpen Patel declare no conflicts of interest.

with pneumonitis incidence. At thresholds of 100% sensitivity and 65–91% specificity corresponding to maximum prediction accuracy for pneumonitis, these parameters had the following cutoff values: MLD = 13.6 $GyEQD2_{Lung}$, V20 = 25%, pMLD = 13.2 $GyEQD2_{Lung}$, pV20 = 15%, pF20 = 17%, sF20 = 25%. Significant parameters MLD, V20, pF20, and sF20 were not cross-correlated to significant parameters pMLD and pV20, indicating that they may offer independently predictive information (Spearman $\rho < 0.7$).

Conclusions: We reported differences in anatomic and functional lung dosimetry between patients with and without pneumonitis in this limited patient cohort. Adding selected independent functional lung parameters may risk stratify patients for pneumonitis. Validation studies are ongoing in a prospective functional lung avoidance trial at our institution.

Keywords

Computed tomography; Radiotherapy; SPECT; PET; Sequelae; Toxicity

Introduction

Radiation induced pulmonary toxicity is a common and clinically significant issue in patients undergoing definitive radiotherapy to the thorax, with incidence rates as high as 30% and fatal toxicity in up to 2% of patients.[1,2] Multiple clinical factors such as patient age, baseline tumor size, and concurrent chemotherapy regimen have been explored for correlation to pneumonitis occurrence, but previous studies have not been able to provide a practical method by which to both identify high risk patients and mitigate that risk.[2,3] Dose-volume parameters and anatomic lung constraints are the current clinical standards used to mitigate pneumonitis risk – most notably the volume of lung receiving >20 Gy (V_{20Gy}) and mean lung dose (MLD). However, constraints of V20 <20%, still resulted in an 18.4% risk of clinical grade pneumonitis.[2] A pooled analysis of correlation between mean lung dose and clinical grade pneumonitis reported an overall rate of 10% in lung cancer patients, but rates between centers varied from 3–13%.[4] The risk of pneumonitis is thought to be a major limiting factor to the dose that can be safely delivered to lung cancers that are at high risk for local failure.

Several imaging modalities exist for assessing lung function and identifying avoidance regions during radiotherapy planning to mitigate risk of pulmonary toxicity. Single photon emission computed tomography (SPECT) perfusion and ventilation imaging have been shown by multiple centers to provide sensitive measures of regional lung function.[5, 6] It is unclear whether SPECT ventilation or perfusion imaging is superior in predicting pneumonitis. Recent investigations using [^{68}Ga]MAA and [^{68}Ga]Galligas PET/CT tracers for enhanced resolution perfusion and ventilation mapping have shown reduced dose to functional lung when adapting plans to perfused but not ventilated lung.[7]

An alternative modality in the form of 4DCT ventilation imaging defined comparable areas of functional lung to SPECT ventilation scans for functional lung avoidance planning,[8, 9] without subjecting patients to additional radiation dose.[10] However, 4DCT ventilation maps are derived from Jacobian transformation matrices that deformably register peak-inhale and end-exhale phases, a process that adds sources of uncertainty.[11, 12] High spatial and temporal

resolution non-ionizing ^{3}He MRI was shown in COPD patients to identify regions that correlated well with ventilation defects and emphysematous morphology and was demonstrated to be safe in elderly and respiratory compromised patients.[13, 14]

A more commonly available approach for assessing the inflammatory component of radiation pneumonitis comes from FDG PET imaging.[15] Uptake of FDG serves as a biomarker of leukocytic presence and activity, namely eosinophilic airway inflammation in asthma patients.[16] Given that the lung is in contact with external air and engages in active immune surveillance, observed physiologic FDG uptake in normal functional lung may be caused in part by increased lymphatic flow. Lymph cells that depend on anaerobic glycolysis (e.g., granulocytes and lymphocytes) accumulate high levels of [^{18}F]-FDG.[16] Further interrogation of baseline descriptors of FDG PET uptake heterogeneity in lung parenchyma may shed light on physiologic and mechanistic underpinnings of patients with predisposition for developing pneumonitis.

Candidate predictors of pneumonitis across functional lung imaging modalities are widespread and variable in definition. In addition to conventional anatomic mean lung dose (MLD), SPECT perfusion-weighted and SPECT ventilation-weighted values of the MLD and V20 were found to be significantly higher in patients developing pneumonitis versus those who do not.[17] Predictors using 4DCT ventilation included the volume of functional lung with greater than 84% of maximum ventilation receiving greater than 20 Gy.[18] Metrics derived from pre-treatment FDG PET scans that correlated with pneumonitis outcome after radiotherapy include SUV_{mean},[19] SUV standard deviation,[20] the 95th percentile of FDG uptake in the lungs,[21, 22] and the SUV ratio of irradiated lung tissues compared with that of non-irradiated lung tissues.[23] An increase in FDG uptake during the first 2 weeks of RT has been described as predictive for pneumonitis.[24] SUV_{mean} and Global Lung Parenchymal Glycolysis (GLPG) also significantly increased following RT.[25]

We have previously introduced a framework for extracting dose-volume and dose-function parameters from SPECT perfusion scans as candidate predictors of pneumonitis, including mean lung dose to highly perfused areas above 70% of maximum perfusion (pMLD).[26] The purpose of this investigation was to apply our framework to both perfusion SPECT/CT and FDG PET/CT imaging in order to extract candidate predictors of radiation pneumonitis from baseline lung function heterogeneity and functional lung dosimetry. We compared a select set of multimodality functional lung imaging and dosimetric parameters reported in the literature as candidate pneumonitis predictors while minimizing the influence of false discoveries.

Materials and methods

Patient characteristics

The framework for functional lung delineation and dose-function metric extraction we have previously described was applied to a cohort of 28 patients with the approval of the University of Washington Institutional Review Board (IRB).[26] All patients receiving definitive thoracic radiation from 2013–2015 with either a lung primary or metastatic disease to the lungs and pre-treatment perfusion [^{99m}Tc]MAA SPECT/CT were included.

The clinical characteristics of the patients were collected and are further described in Table 1. All patients had at least 6 months follow-up, 13 of whom had at least 1 year follow-up. Patients were typically seen at least once every 3 months, with toxicity assessment at each visit. Pulmonary morbidity was graded by the National Cancer Institute's Common Terminology Criteria for Adverse Events version 4 (CTCAE v4) for pneumonitis. Patients were dichotomized for pulmonary toxicity based on presence or absence of grade ≥ 2 pneumonitis (GR2+ PNM), defined by CTCAE v4 as the clinical indication for prednisone administration. All GR2+ PNM events were observed prior to 6 months post-treatment.

SPECT/CT and PET/CT image processing

Pre-treatment [^{99m}Tc]MAA perfusion SPECT/CT scans were co-registered to planning 4DCT scans in 28 patients who received definitive-dose thoracic radiotherapy. All patients underwent pre-treatment [^{99m}Tc]MAA SPECT/CT scans during which they were immobilized in radiation treatment position. SPECT/CT images were acquired on a Precedence™ (Philips Healthcare, Cleveland, OH) dual head gamma camera 16 slice CT scanner. A fixed intravenous injected dose was followed immediately by time-averaged SPECT acquisition (64 views, 20 sec/view, 180 degree arc). Emission images were corrected for scatter, collimator-detector distance, and attenuation using a helical CT to promote semi-quantitative reproducibility. Reconstructions were performed with the Astonish™ (Philips Healthcare, Cleveland, OH) ordered subset expectation-maximization (OSEM) iterative algorithm that incorporates spatial resolution recovery. Images were reconstructed on 4.64 mm isotropic grids with a 10 mm cutoff Hanning filter.

Twenty-five patients underwent pre-treatment [^{18}F]FDG PET/CT scans that were co-registered to the same planning CT scans. The majority of scans (n = 21) were completed with patients immobilized in treatment position, while the remaining scans (n = 4) were conducted as whole body treatment planning scans. PET/CT images were acquired on a Discovery STE™ (GE Healthcare, Waukesha, WI) scanner. Administration of a weight-based injection was followed by a standard 60 min uptake period (nominal). PET images were acquired for 5 min per axial field-of-view and reconstructed with OSEM onto 5.47 × 5.47 × 3.27 mm^3 voxel grid with post-reconstruction Gaussian filtration.

All scans were rigidly co-registered to avoid introducing unwanted variability due to deformable registration. CT-CT rigid transformations were subsequently applied to low-resolution functional imaging modalities under time-averaged and free-breathing acquisitions. Rigid alignment of FDG PET and MAA SPECT images conservatively preserved image intensity distributions, from which quantitative metrics were extracted. In the case of SPECT, the associated helical CT scans acquired at end-exhale were co-registered to the end-exhale phases of 4DCT treatment planning scans. In the case of FDG PET, the associated CT scans were not consistently acquired at end-exhale phase, requiring alignment of these scans to the 4DCT phase-averaged images.

Defining anatomic and functional lung contours

Tumor-subtracted total lung contours were used to extract functional lung parameters. FDG PET scans display a heterogeneous distribution of low (~2 SUV) values throughout

functional lung, but high values near tumor (>10 SUV) that spill into areas of functional lung from resolution-limited partial volume errors. To prevent areas of high uptake near tumor or heart from being interpreted falsely as high uptake in functional lung, the gradient search PET Edge tool in MIM version 6.6™ (MIM Software Inc., Cleveland, OH) was applied iteratively to reproducibly expand the tumor and heart boundaries as much as necessary to include all FDG avid areas. A visual inspection was then performed to ensure subtraction of any remaining tumor or heart uptake rims.

We defined functional lung volumes using a technique that we have previously reported on.[26] In brief, we defined highly functional lung as the 70% threshold of maximum perfusion and 70% of maximum FDG uptake (SUV_{max}) similar to another investigation.[21] Function was normalized to the aortic arch for SPECT/CT perfusion contours and total SUV counts in the entire tumor-subtracted lung for FDG PET/CT contours. The median (range) of highly perfused lung volumes was 76 cm^3 (14 – 262 cm^3, 1–9% of total lung), while the median (range) of FDG-avid lung volumes was 84 cm^3 (8 – 530 cm^3, 1–28% of total lung). From these functional regions we were able to extract dosimetric parameters as candidate predictors. Normal lung doses were converted to biologically equivalent voxel dose distributions in 2 Gy fraction sizes ($EQD2_{Lung}$) using the linear-quadratic model for a clinical endpoint of pneumonitis ($\alpha/\beta = 3$) in order to account for fractionation variability as well as radiobiological effectiveness of different radiation modalities.[27]

Candidate predictors of pneumonitis

Several classes of imaging and dosimetric candidate predictors selected based on prior published work are listed in Table 2. Conventional parameters included anatomic MLD and V20 which have been shown to significantly associate with pneumonitis.[2] Baseline functional imaging predictors were assessed by intensity histogram distribution moments (coefficient of variation, skewness, kurtosis) using the MIM 6.5 statistics function. In the case of PET, SUV_{mean} and Global Lung Parenchymal Glycolysis (GLPG) were also extracted.[25] SUV_{mean} was selected over SUV_{max}, which has been shown to not be significantly increased in patients developing pneumonitis.[24] GLPG is the functional lung equivalent of tumor Total Lesion Glycolysis and is described by the following equation:

$$GLPG = SUV_{mean} * (Tumor\ subtracted \quad Lung \quad Volume) \quad (1)$$

Baseline functional imaging predictors were selected based on physiological rationales. For example, a given patient's baseline functional lung distribution showing positive skewness may have a physiological correlate of low proportions of lung with high function (quantified by normalized counts for SPECT perfusion), which may be present in a patient with areas of emphysematous lung. Patients with skewed functional lung distributions may be hypothesized to be at increased risk for pneumonitis, given that they have less functional reserve. In another example, a high SUV_{mean} may have a physiological correlate of a high proportion of lung with greater numbers of circulating or resident immune cells, given that high FDG uptake is seen in FDG PET scans not only in areas of high metabolic activity but

also in areas of active infection. In other words, a higher SUV_{mean} may indicate an immune microenvironment that is more prone to provocation into radiation pneumonitis.

Three types of functional lung dosimetric parameters were evaluated from MAA SPECT perfusion (PERF) or FDG PET (SUV). Perfusion-derived metrics begin with the prefix "p," while those derived from FDG PET begin with the prefix "s":

(1) mean dose to highly functional lung (PERF: pMLD, SUV: sMLD), as described in our previous work where pMLD was found to be significantly correlated with pneumonitis (AUC = 0.93).[26]

(2) volume of highly functional lung (PERF: pV20, SUV: sV20) receiving 20 Gy or higher, similar in concept to the metric described by Faught et al (2017).[18] Although those authors defined highly functional lung as the 84th ventilation percentile, we use the 70% threshold to remain consistent with our previous work.

(3) dose-function histogram quantiles (PERF: pF20, SUV: sF20), defined as the fraction of integral lung function receiving 20 Gy or higher. Total perfusion counts or SUV in regions receiving above 20 Gy were normalized by the total perfusion counts or total SUV in the entire tumor-subtracted lung.

Lastly, clinical risk factors for pneumonitis identified by Palma et al. (2013), such as age and concurrent chemotherapy, were evaluated as potential confounders to the imaging and dosimetric candidate predictors.[2] Other clinical factors listed in Table 1 that captured patient heterogeneity, including but not limited to treatment modality and treatment history, were also considered for association to pneumonitis.

Statistical analysis

Univariate logistic regression area-under-the-curve (AUC) was calculated for each clinical risk factor's association to GR2+ PNM. Mann-Whitney and Fisher exact tests of differences in clinical risk factors between patients who presented with GR2+ PNM and those who did not were performed. Non-parametric empirical receiver operating characteristic (ROC) curves tested the predictive accuracy of the imaging and dosimetric features listed in Table 2 for incidence of GR2+ PNM. Parameters were considered statistically significant if the two-tailed asymptotic p-value for the AUC (null hypothesis AUC = 0.5) was less than 0.05. A further Benjamini-Hochberg correction was applied to all resulting p-values (Mann-Whitney, Fisher exact, ROC) to correct for false discoveries associated with multiple comparisons, accepting a false discovery rate of 5%. Factors that remained statistically significant after this correction are highlighted in gray in the final column of Table 4. Multivariate statistical testing was not performed due to small sample size and a limited number of pneumonitis events (5). Cutoff values for each significant parameter were calculated at an operating point that maximized the Youden index (sensitivity + specificity – 1) for discriminating patients according to GR2+ PNM status (Table 5). Rank (Spearman) correlation coefficients were calculated as measures of inter-parameter cross-correlation for individual predictors of GR2+ PNM (Figure 1).

Results

Comparing pneumonitis and non-pneumonitis cases

Patients receiving concurrent chemotherapy trended towards elevated risk for GR2+ PNM (AUC = 0.77, $p = 0.05$). The remaining clinical risk factors in Table 3 did not associate with statistically significant differences in incidence of GR2+ PNM ($p \geq 0.25$). Anatomic mean lung dose was significantly higher in GR2+ PNM patients (14.6 vs 9.3 Gy $EQD2_{Lung}$, $p = 0.013$). Pneumonitis patients also demonstrated significantly higher pMLD (19.3 vs 5.6 Gy $EQD2_{Lung}$, $p = 0.048$) and a trend towards a difference in sMLD (22.3 vs. 8.8 Gy $EQD2_{Lung}$, $p = 0.057$).

Correlation of candidate predictors with pneumonitis

Anatomic mean lung dose (AUC = 0.94, $p = 0.013$) and V20 (AUC = 0.96, $p = 0.013$) were both predictive of GR2+ PNM under univariate logistic regression. Baseline heterogeneity and lung function/volume metrics were not predictive (AUC < 0.66). Several lung perfusion dosimetric parameters correlated with GR2+ PNM: pMLD (AUC = 0.84, $p = 0.047$), pV20 (AUC = 0.86, $p = 0.041$), and pF20 (AUC = 0.87, $p = 0.041$). One FDG PET dosimetric parameter, sF20 (AUC = 0.97, $p = 0.013$), was found to have strong correlation with GR2+ PNM. sMLD failed to reach significance following correction for multiple comparisons (Table 4).

Selecting threshold values for significant predictors of pneumonitis

From the statistically significant univariate predictors in Table 4, thresholds that maximized the Youden index to stratify patients at high risk for pneumonitis included MLD > 13.6 $GyEQD2_{Lung}$, V20 > 25%, pMLD > 13.2 $GyEQD2_{Lung}$, pV20 > 14%, pF20 > 17%, and sF20 > 25% (Table 5). Youden thresholds corresponded to operating points with 100% sensitivity and > 65% specificity, which represent conservative dosimetric constraints that guard against false negative predictions.

Cross-correlation between significant parameters testing independence of information

Spearman rank correlation coefficients between anatomic and functional lung dosimetric parameters that were GR2+ PNM predictors, taken from Table 4, are listed and visualized as a false red-white color map in Figure 1. Anatomic MLD correlated strongly with the other anatomic parameter, V20 ($\rho = 0.93$), and also with functional parameters pF20 ($\rho = 0.86$) and sF20 ($\rho = 0.94$). Similarly, anatomic V20 correlated strongly with anatomic MLD ($\rho = 0.93$) and with the functional parameters pF20 ($\rho = 0.91$) and sF20 ($\rho = 0.97$). Functional lung dose-volume metrics with weak cross-correlation to anatomic parameters (MLD, V20) were pMLD ($\rho = 0.59, 0.52$) and pV20 ($\rho = 0.56, 0.56$), suggesting complementarity of predictive information.

Discussion

Our previously published work outlined a framework for identifying metrics associated with GR2+ PNM outcome, including both anatomic MLD and functional pMLD as potential candidate predictors.[26] This paper applied that framework and extended it to a suite of pre-

treatment functional lung heterogeneity metrics alongside anatomic and functional lung dosimetric parameters for correlation with GR2+ PNM. This study is the first to report on functional lung heterogeneity and functional lung dosimetry in the same cohort, as well as the first to directly compare FDG PET and SPECT perfusion metrics. In this expanded cohort relative to our previous analysis and upfront false discovery rate correction, pMLD remained correlated to pneumonitis outcome (AUC = 0.84, $p = 0.048$).[26] Anatomic MLD also retained correlation to GR2+ PNM incidence (AUC = 0.94, $p = 0.013$). Our metric with the greatest predictive capacity for GR2+ PNM was the functional parameter sF20 (AUC = 0.97). This was followed by anatomic V20 (AUC = 0.95), anatomic MLD (AUC = 0.94), and three functional dosimetric factors: pF20 (AUC = 0.87), pV20 (AUC 0.86) and pMLD (AUC = 0.84).

In the context of pre-existing emphysematous lungs in over half of our patient cohort, we hypothesized that baseline functional lung heterogeneity would be a significant predictive factor of radiation pneumonitis. However, none of our selected descriptors of baseline heterogeneity alone without dosimetric information correlated significantly with GR2+ PNM. Anatomic and functional lung dosimetry had greater significance than baseline patient characteristics, including clinical risk factors (age, concurrent chemotherapy, prior thoracic radiation therapy) and baseline functional lung parameters (perfusion and FDG uptake heterogeneity) for predicting who is at highest risk for developing pneumonitis. These findings add to the growing evidence that anatomic/functional dosimetry beyond baseline characteristics, clinical or functional, may be most critical for predicting pneumonitis risk. Based on our findings, dose to highly perfused lung may be more important than dose to FDG-avid lung in predicting GR2+ PNM. All three of our perfusion metrics correlated significantly with GR2+ PNM, whereas only one FDG-PET metric (sF20) did. Although sF20 had the highest AUC under ROC analysis of all dose-function or dose-volume parameters, this metric was highly correlated with both anatomic MLD and V20 ($\rho > 0.93$).

The strength of correlation between metrics sheds light on which factors could be selected and combined in a multivariate model to maximize predictive accuracy for GR2+ PNM. High correlation between any two given metrics in our cohort such as anatomic MLD and sF20 ($\rho = 0.94$) indicates that, in a multivariate model, including both metrics would be unlikely to add predictive power. This logic also applies to the observed high correlation between sF20 and pF20 ($\rho = 0.90$). In contrast, combining two metrics such as MLD with pMLD, or V20 and pV20 may produce a multivariate model with enhanced predictive power given the low inter-parameter cross-correlation ($\rho < 0.59$). Following this analysis, independently predictive functional lung parameters could be combined to form a pneumonitis risk signature.

Multiple studies have indicated in lung and esophageal cancer patients that elevated non-target pre-treatment lung FDG uptake correlates with increased risk of GR2+ PNM after radiotherapy.[19, 20, 22, 23] Anthony et al. (2017) report on a study of 96 esophageal cancer patients in which the SUV standard deviation had an AUC of 0.69, and when added to a single texture feature improved classifier performance on average by up to 0.08 in a logistic regression model predicting GR2+ PNM.[20] In our study, however, the SUV coefficient of variation on baseline FDG PET imaging (which includes SUV standard deviation), was not a

significant predictor of pneumonitis (AUC 0.36, $p = 0.55$). Chaudhuri et al. (2016) report that, in a retrospective review of 258 lung cancer patients (28 with GR2+ PNM), mean lung SUV > 0.56 on pre-treatment FDG PET was associated with higher risk of pneumonitis (AUC = 0.74, sensitivity 82.1%, specificity 57.9%). SUV_{mean} did not correlate with PNM outcome in our cohort (AUC 0.54, $p = 0.81$).[19]

Our cohort does, however, show stronger correlation between our discovered anatomic and functional dosimetry to GR2+ PNM than other groups, including those utilizing 4DCT. Vinogradsky et al. (2013), in their use of 4DCT based ventilation scans, report an AUC of 0.58 for anatomic mean lung dose and 0.62 for dose-function metrics, compared to an AUC > 0.84 for MLD, V20, pMLD, pV20, pF20, and sF20 in our study.[28] Given the larger patient cohort (96 lung cancer patients) in the Vinogradsky study, we attribute these discrepancies in part to differences in patient population, functional imaging modality (4DCT-derived ventilation), image registration technique, and treatment planning approaches. Faught et al. (2017) similarly report AUC > 0.7 for fV10Gy, fV20Gy, and fMLD of thirty lung cancer patients retrospectively re-planned using 4DCT ventilation based mapping.[29] In addition to pneumonitis, 4DCT functional volume-based models have predicted radiation fibrosis (AUC = 0.85).[30] The large number of different functional lung metrics reported across multiple studies raises the need for standardization of variable definitions, as well as harmonization of the method by which images are acquired, reconstructed and processed across institutions. Given that Faught et al. show correlation of GR2+ PNM incidence with functional V20 using 4DCT ventilation imaging, while we were able to show correlation with functional V20 using SPECT perfusion imaging, we would recommend standardization and harmonization of functional V20 parameters.

An ongoing prospective phase II trial at our institution (NCT02773238) will validate our findings, as part of a strategy to mitigate pulmonary toxicity risk through delivery of functional lung avoidance and response-adaptive escalation (FLARE) RT in patients with locally advanced NSCLC.[31] The ongoing trial consists of longitudinal SPECT/CT perfusion and FDG PET/CT imaging that will validate whether multiple functional lung parameters improve prediction over a single parameter, and establish which set of parameters are most important to assess in individual patients. Our observational study suggests that dose-function metrics derived from SPECT perfusion scans may outperform those derived from FDG PET. Multiple prospective functional lung avoidance clinical trials are also underway to validate 4DCT ventilation (NCT02528942) and ^{3}He MRI (NCT02002052) candidate pneumonitis predictors.

This study is limited by multiple factors. First, the expanded cohort is still small with few (5) pneumonitis events. We acknowledge that our cohort size may lack sensitivity for detection of statistical significance in some of our investigated metrics, including baseline FDG heterogeneity features given previously published works suggesting the importance of baseline FDG uptake.[20] However, a possible interpretation of our results is that perfused lung dose-volume and dose-function metrics such as pMLD, pV20, and pF20 are better predictors of pneumonitis risk than FDG PET metrics. Given our small patient cohort, we did not perform multivariate testing, extract additional image texture features of baseline functional lung, or deploy large-scale machine learning techniques. Second, given the

variability of treatment planning PET scans which were not all performed with custom immobilization, the study may have had limited ability to identify additional FDG PET predictors of GR2+ PNM. However, these factors will be prospectively investigated in the FLARE RT trial with standardized PET scans at pre, mid, and post-treatment, during which all patients are scanned in treatment position. Third, our patient population remains heterogeneous since our previous study, including a range of tumor and treatment characteristics. We also had potential competing clinical risk factors for pneumonitis such as concurrent chemotherapy, prior radiotherapy, and patient age, though none were significantly different between pneumonitis and non-pneumonitis subgroups. Variable tumor etiology precluded this study from investigating tumor response to radiation as an additional candidate predictor. Furthermore, diversity in radiation treatment modality and fractionation pattern imposed calculations of equivalent dose. An $EQD2_{Lung}$ dose of 13.6 Gy, as reported for our anatomic MLD significant predictor of GR2+ PNM, would be equivalent to 19.3 Gy physical dose assuming standard fractionation (60 Gy, 2 Gy per fraction). These and other methods may promote standardization of anatomic and functional lung dosimetry across institutions to guide functional lung avoidance during radiation treatment planning.

Conclusions

Anatomic lung dose, functional lung dose-volume and dose-function histogram parameters were statistically associated with incidence of CTCAE grade 2 or higher radiation pneumonitis. We confirmed two anatomic dose parameters (MLD, V20), and four functional dose parameters (pMLD, pV20, pF20, sF20) as significant univariate predictors of pneumonitis in this dataset. Validation of the perfused lung planning constraints we describe is underway within a prospective functional lung avoidance trial.

Acknowledgements:

This work was funded by the Radiological Society of North America (RMS1622) and NIH/NCI R01CA204301

References

1. Mehta V Radiation pneumonitis and pulmonary fibrosis in non-small-cell lung cancer: pulmonary function, prediction, and prevention. Int J Radiat Oncol Biol Phys. 2005;63(1):5–24. [PubMed: 15963660]
2. Palma DA, Senan S, Tsujino K, et al. Predicting radiation pneumonitis after chemoradiation therapy for lung cancer: an international individual patient data meta-analysis. Int J Radiat Oncol Biol Phys. 2013;85(2):444–450. [PubMed: 22682812]
3. Zhao J, Yorke ED, Li L, et al. Simple Factors Associated With Radiation-Induced Lung Toxicity After Stereotactic Body Radiation Therapy of the Thorax: A Pooled Analysis of 88 Studies. Int J Radiat Oncol Biol Phys. 2016;95(5):1357–1366. [PubMed: 27325482]
4. Kwa SL, Lebesque JV, Theuws JC, et al. Radiation pneumonitis as a function of mean lung dose: an analysis of pooled data of 540 patients. Int J Radiat Oncol Biol Phys. 1998;42(1):1–9. [PubMed: 9747813]
5. Shioyama Y, Jang SY, Liu HH, et al. Preserving functional lung using perfusion imaging and intensity-modulated radiation therapy for advanced-stage non-small cell lung cancer. Int J Radiat Oncol Biol Phys. 2007;68(5):1349–1358. [PubMed: 17446001]
6. Yaremko BP, Guerrero TM, Noyola-Martinez J, et al. Reduction of normal lung irradiation in locally advanced non-small-cell lung cancer patients, using ventilation images for functional avoidance. Int J Radiat Oncol Biol Phys. 2007;68(2):562–571. [PubMed: 17398028]

7. Siva S, Thomas R, Callahan J, et al. High-resolution pulmonary ventilation and perfusion PET/CT allows for functionally adapted intensity modulated radiotherapy in lung cancer. Radiother Oncol. 2015;115(2):157–162. [PubMed: 25935743]
8. Yamamoto T, Kabus S, Lorenz C, et al. Pulmonary ventilation imaging based on 4-dimensional computed tomography: comparison with pulmonary function tests and SPECT ventilation images. Int J Radiat Oncol Biol Phys. 2014;90(2):414–422. [PubMed: 25104070]
9. Kida S, Bal M, Kabus S, et al. CT ventilation functional image-based IMRT treatment plans are comparable to SPECT ventilation functional image-based plans. Radiother Oncol. 2016;118(3): 521–527. [PubMed: 26922488]
10. Waxweiler T, Schubert L, Diot Q, et al. A complete 4DCT-ventilation functional avoidance virtual trial: Developing strategies for prospective clinical trials. J Appl Clin Med Phys. 2017;18(3):144–152.
11. Persson GF, Nygaard DE, Munck Af Rosenschold P, et al. Artifacts in conventional computed tomography (CT) and free breathing four-dimensional CT induce uncertainty in gross tumor volume determination. Int J Radiat Oncol Biol Phys. 2011;80(5):1573–1580. [PubMed: 21163584]
12. Castillo E, Castillo R, Vinogradskiy Y, Guerrero T. The numerical stability of transformation-based CT ventilation. Int J Comput Assist Radiol Surg. 2017;12(4):569–580. [PubMed: 28058533]
13. Capaldi DP, Sheikh K, Guo F, et al. Free-breathing pulmonary 1H and Hyperpolarized 3He MRI: comparison in COPD and bronchiectasis. Acad Radiol. 2015;22(3):320–329. [PubMed: 25491735]
14. Fain S, Schiebler ML, McCormack DG, Parraga G. Imaging of lung function using hyperpolarized helium-3 magnetic resonance imaging: Review of current and emerging translational methods and applications. J Magn Reson Imaging. 2010;32(6):1398–1408. [PubMed: 21105144]
15. Tsoutsou PG, Koukourakis MI. Radiation pneumonitis and fibrosis: mechanisms underlying its pathogenesis and implications for future research. Int J Radiat Oncol Biol Phys. 2006;66(5):1281–1293. [PubMed: 17126203]
16. Harris RS, Venegas JG, Wongviriyawong C, et al. 18F-FDG uptake rate is a biomarker of eosinophilic inflammation and airway response in asthma. J Nucl Med. 2011;52(11):1713–1720. [PubMed: 21990575]
17. Hoover DA, Reid RH, Wong E, et al. SPECT-based functional lung imaging for the prediction of radiation pneumonitis: a clinical and dosimetric correlation. J Med Imaging Radiat Oncol. 2014;58(2):214–222. [PubMed: 24373453]
18. Faught AM, Yamamoto T, Castillo R, et al. Evaluating which dose-function metrics are most critical for functional-guided radiotherapy with CT ventilation imaging. Int J Radiation Oncol Biol Phys. 2017 3 30; Epub ahead of print
19. Chaudhuri AA, Binkley MS, Rigdon J, et al. Pre-treatment non-target lung FDG-PET uptake predicts symptomatic radiation pneumonitis following Stereotactic Ablative Radiotherapy (SABR). Radiother Oncol. 2016;119(3):454–460. [PubMed: 27267049]
20. Anthony GJ, Cunliffe A, Castillo R, et al. Incorporation of pre-therapy 18 F-FDG uptake data with CT texture features into a radiomics model for radiation pneumonitis diagnosis. Med Phys. 2017.
21. Petit SF, van Elmpt WJ, Oberije CJ, et al. [(1)(8)F]fluorodeoxyglucose uptake patterns in lung before radiotherapy identify areas more susceptible to radiation-induced lung toxicity in non-small-cell lung cancer patients. Int J Radiat Oncol Biol Phys. 2011;81(3):698–705. [PubMed: 20884128]
22. Castillo R, Pham N, Ansari S, et al. Pre-radiotherapy FDG PET predicts radiation pneumonitis in lung cancer. Radiat Oncol. 2014;9:74. [PubMed: 24625207]
23. Zhang Y, Yu Y, Yu J, Fu Z, Liu T, Guo S. 18FDG PET-CT standardized uptake value for the prediction of radiation pneumonitis in patients with lung cancer receiving radiotherapy. Oncol Lett. 2015;10(5):2909–2914. [PubMed: 26722262]
24. De Ruysscher D, Houben A, Aerts HJ, et al. Increased (18)F-deoxyglucose uptake in the lung during the first weeks of radiotherapy is correlated with subsequent Radiation-Induced Lung Toxicity (RILT): a prospective pilot study. Radiother Oncol. 2009;91(3):415–420. [PubMed: 19195730]

25. Abdulla S, Salavati A, Saboury B, Basu S, Torigian DA, Alavi A. Quantitative assessment of global lung inflammation following radiation therapy using FDG PET/CT: a pilot study. Eur J Nucl Med Mol Imaging. 2014;41(2):350–356. [PubMed: 24085504]

26. Dhami G, Zeng J, Vesselle HJ, et al. Framework for radiation pneumonitis risk stratification based on anatomic and perfused lung dosimetry. Strahlenther Onkol. 2017;193(5):410–418. [PubMed: 28255667]

27. Borst GR, Ishikawa M, Nijkamp J, et al. Radiation pneumonitis after hypofractionated radiotherapy: Evaluation of the LQ(L) model and different dose parameters. Int J Radiat Oncol Biol Phys. 2010;77(5):1596–1603. [PubMed: 20231066]

28. Vinogradskiy Y, Castillo R, Castillo E, et al. Use of 4-dimensional computed tomography-based ventilation imaging to correlate lung dose and function with clinical outcomes. Int J Radiat Oncol Biol Phys. 2013;86(2):366–371. [PubMed: 23474113]

29. Faught AM, Miyasaka Y, Kadoya N, et al. Evaluating the Toxicity Reduction with CT-Ventilation Functional Avoidance Radiotherapy. Int J Radiat Oncol Biol Phys. 2017 4 26; Epub ahead of print.

30. Lan F, Jeudy J, Senan S, et al. Should regional ventilation function be considered during radiation treatment planning to prevent radiation-induced complications? Med Phys. 2016;43(9):5072. [PubMed: 27587037]

31. Lee E, Zeng J, Miyaoka RS, et al. Functional lung avoidance and response-adaptive escalation (FLARE) RT: multimodality plan dosimetry of a precision radiation oncology strategy. Med Phys. 2017.

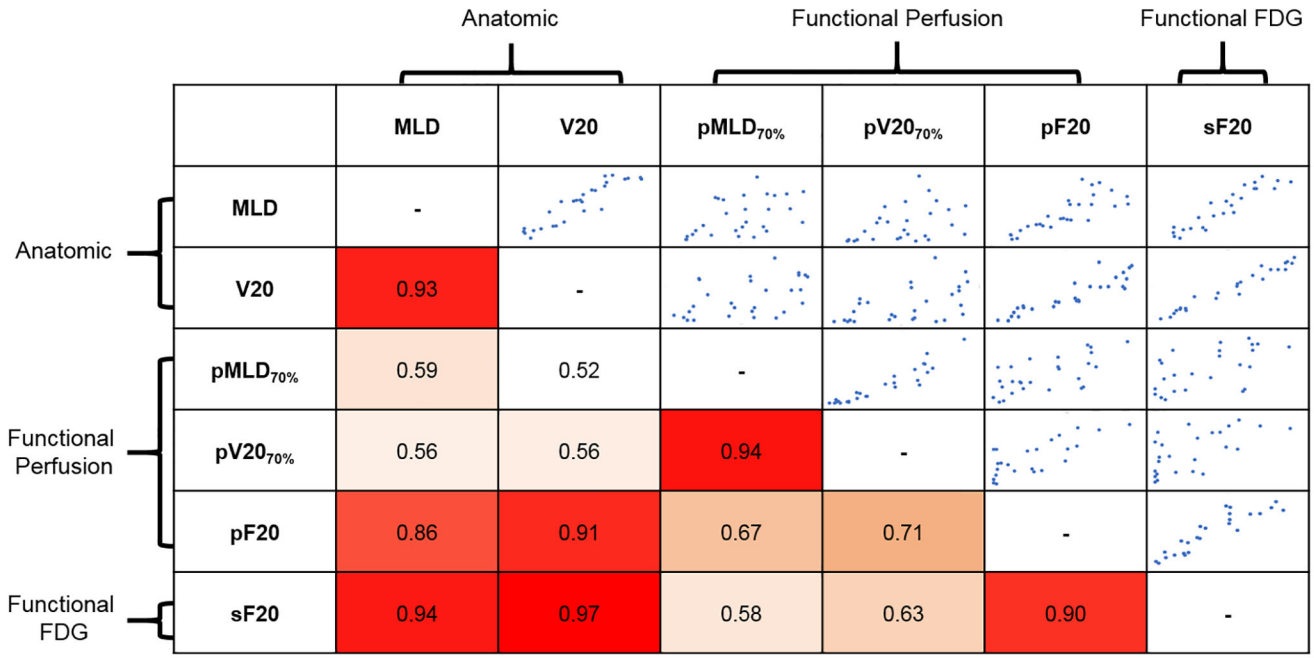

Figure 1: Inter-parameter Spearman rank correlation coefficients for predictors of GR2+ PNM.

White indicates low correlation. Orange indicates moderate correlation. Red indicates strong correlation. Anatomic dose parameters MLD and V20 correlate strongly with each other. Both also correlate strongly with pF20 and sF20. pMLD and pV20 correlate strongly with each other but not with anatomic dosimetry. Scatter plots in the upper diagonal represent the pairwise relationship between variables that intersect in each cell to provide a visual representation of the strength of correlation mirrored across the diagonal.

Table 1:

Patient characteristics

Characteristic	N (%)	Without GR2+ pneumonitis (N = 23)	With GR2+ pneumonitis (N = 5)
Age at time of radiation treatment (years)	Median: 70.5 Range: 53–81	Median: 75 Range: 53–80	Median: 67 Range: 55–81
Sex			
Male	11 (39)	8	3
Female	17 (61)	15	2
Clinical stage			
Limited stage SCLC	5 (18)	4	1
I NSCLC	5 (18)	4	1
II NSCLC	1 (4)	0	1
IIIA NSCLC	4 (14)	3	1
IIIB NSCLC	4 (14)	4	0
Locally recurrent	5 (18)	4	1
Metastatic to lung	4 (14)	4	0
Histology			
NSCLC	20 (71)	16	4
SCLC	5 (18)	4	1
Other (other primary)	3 (11)	3	0
Prior thoracic radiation			
Yes	6 (21)	6	0
No	22 (79)	17	5
Concurrent chemotherapy			
Yes	10 (36)	6	4
No	18 (64)	17	1
EQD2 radiation dose (Gy)	Median: 60 Range: 48–66.6	Median: 66 Range: 60–66.6	Median: 60 Range: 48–66.6
Radiation treatment technique			
3D CRT	1 (4)	1	0
IMRT/VMAT	10 (36)	7	3
SBRT	7 (24)	7	0
PBT	10 (36)	8	2
Smoking status			
Lifetime nonsmoker	5 (18)	4	1
Former	19 (68)	15	4
Current	4 (14)	4	0
Pre-existing emphysema			
Yes	14 (50)	12	2
No	14 (50)	11	3

SCLC small cell lung cancer, NSCLC non-small cell lung cancer, EQD2 equivalent dose in 2 Gy per fraction, 3D CRT three-dimensional conformal radiation therapy, IMRT/VMAT intensity-modulated radiotherapy/volumetric modulated arc therapy, SBRT stereotactic body radiation therapy, PBT proton beam therapy

Table 2:

Selected imaging and dosimetric parameters investigated by this study based on previous findings.

Anatomic Dosimetry	Functional Baseline FDG	Functional Baseline PERF	Functional FDG Dosimetry	Functional PERF Dosimetry
MLD[a]	SUV_{mean}[b]	-	sMLD	pMLD[c]
V20[a]	GLPG	-	sV20[d]	pV20[d]
	COV	COV	sF20	pF20
	Skewness	Skewness		
	Kurtosis	Kurtosis		

Resources referred to,

[a] = Palma et al 2013,

[b] = De Ruysser et al 2009,

[c] = Dhami et al 2017,

[d] = Faught et al 2017.

pMLD, sMLD, pV20, and sV20 are taken at the 70% perfusion and SUV_{max} thresholds.

Table 3:

Univariate clinical risk factor association with incidence of grade 2 or higher pneumonitis.

Clinical Factor	AUC	p-value
Age at time of radiation treatment (years)	0.69	0.25†
Sex (male vs. female)	0.63	0.35‡
Histology (SCLC / other vs. NSCLC)	0.55	0.64‡
Prior thoracic radiation (no vs. yes)	0.63	0.55‡
Concurrent chemotherapy (yes vs. no)	0.77	0.05‡
Radiation treatment technique (PBT vs. IMRT / VMAT / SBRT / 3D-CRT)	0.53	0.83‡
Smoking status (never vs. current / former)	0.51	0.89‡
Pre-existing emphysema (no vs. yes)	0.56	0.62‡

†Mann-Whitney test

‡Fisher exact test

Table 4:

Receiver-operator characteristic (ROC) analysis for selected imaging and dosimetric factors listed in Table 2.

Parameter	AUC	Standard Error	p-value	p-value corrected
Anatomic Dose				
MLD	0.94	0.090	0.0025	0.013
V20	0.96	0.066	0.0016	0.013
Functional Baseline FDG				
SUV_{mean}	0.55	0.18	0.75	0.81
GLPG	0.65	0.14	0.31	0.55
Coefficient of Variation	0.36	0.20	0.34	0.55
Skewness	0.57	0.20	0.63	0.73
Kurtosis	0.58	0.18	0.59	0.72
Functional Baseline PERF				
Coefficient of Variation	0.65	0.11	0.29	0.55
Skewness	0.47	0.16	0.83	0.83
Kurtosis	0.40	0.18	0.49	0.65
Functional Dose FDG				
sMLD	0.83	0.12	0.025	0.057
sV20	0.75	0.14	0.089	0.18
sF20	0.97	0.04	0.0014	0.013
Functional Dose PERF				
pMLD	0.84	0.13	0.018	0.048
pV20	0.86	0.11	0.013	0.041
pF20	0.87	0.11	0.011	0.041

Significant predictors of GR2+ PNM highlighted in gray. sMLD did not remain significant after Benjamini-Hochberg correction for false discovery rate.

Table 5:

ROC operating points of GR2+ PNM predictors that maximized the Youden index (sensitivity + specificity − 1)

Parameter	Cutoff Value	Sensitivity	Specificity
MLD	13.6 $GyEQD2_{Lung}$	100%	91%
V20	25%	100%	91%
pMLD	13.2 $GyEQD2_{Lung}$	100%	74%
pV20	15%	100%	65%
pF20	17%	100%	70%
sF20	25%	100%	85%